

# A biologically plausible model of time-scale invariant interval timing: Supporting Information

Rita Almeida<sup>1</sup> & Anders Ledberg<sup>2</sup>,

<sup>1</sup> Institut d'Investigacions Biomèdiques August Pi i Sunyer (IDIBAPS)

C. Mallorca 183, 08036 Barcelona, Spain

E-mail: ralmeida@clinic.ub.es

<sup>2</sup> Center for Brain and Cognition,

Department of Information and Communication Technologies,

Universitat Pompeu Fabra, C. Tànger 122-140, 08018 Barcelona, Spain

E-mai: anders.ledberg@upf.edu

## 1 The effect of weak temporal correlation in the noise process.

In the one-dimensional generic model (Eq. 7 in the paper) we assumed that the noise process was temporally uncorrelated (so called white noise). To test the effect of having a noise process with temporal correlations we run simulations in which this correlations had the form  $a(h) = 0.985^{200 \cdot (h-1)}$  where  $h$  is lag and has the units of milliseconds. Fig. 1A shows the noise autocorrelation. For  $h > 2$  ms the correlation is essentially zero. Fig. 1B,C show response distributions (time to 80% of the units up) as a function of absolute and relative time respectively. It is clear that the temporally correlated noise does not affect the time-scale invariance. We expect this to be the case whenever the width of the autocorrelation is small in comparison to the time intervals of interest.

## 2 The effect of interactions between the units

Here we will exemplify the general rule (given by Eq. 6 in the paper) for how to modify the activation rates.

### 2.1 All-to-all interactions

In this case the activation rates of the units are the same for all units but this rate depends on the total state of the stop-watch (the number of activated units). If we denote this activation rate by  $p_a(t)$  (“a” for all-to-all) we get the following rule of how to change  $p_a$  as a function of the total number of activated units:

$$p_a(t) = p \left( 1 + w \frac{m(t)}{M} \right). \quad (1)$$

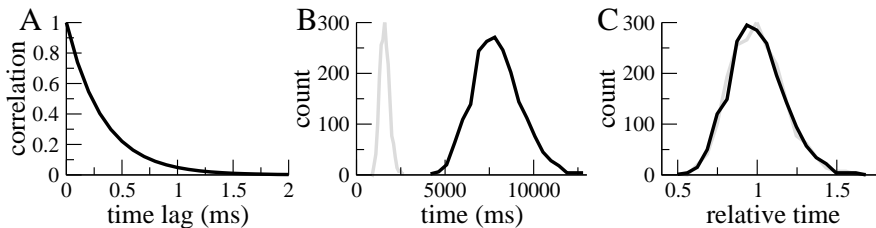


Figure 1: Effect of temporally correlated noise on performance of the 1D model. A: Autocorrelation function of the noise process in Eq. 7 in main paper. B: Response time distributions for two values of the constant term. The gray curve shows the distribution corresponding to  $\mu = -0.009$  and the black that to  $\mu = -0.013$ . C: Same data as in B but after rescaling time. Parameters used:  $M = 50$ ,  $f = 0.8$ ,  $\beta = 0.19$ ,  $\sigma = 0.004$ . Results based on 2000 trials of the stop-watch, for each value of the input. Simulations were run using the explicit Euler method with a step size of 0.005.

Here  $p$  is the baseline activation rate that does not depend on the state of the stop-watch (consistent with the usage in the paper),  $w$  is a small constant measuring the magnitude of the interactions ( $w$  is positive for “excitatory” interactions and negative for “inhibitory”) and  $m(t)$  is the number of activated units at time  $t$ . Note that if  $w = 0$  we are back in the case of non-interacting units. Also note that we could apply any non-linear transformation of  $m(t)$  in Eq. 1 without upsetting the scale invariance.

Intervals of different durations can still be encoded by changing  $p$ , just as in the non-interacting case, but now the mean and standard deviations of  $T_{f,M}$  are given by

$$\begin{aligned} \mathbb{E}[T_{f,M}] &= \frac{1}{p} \sum_{k=0}^{f \cdot M - 1} \frac{1}{(M-k)(1+kw/M)} \\ S[T_{f,M}] &= \frac{1}{p} \left( \sum_{k=0}^{f \cdot M - 1} \frac{1}{[(M-k)(1+kw/M)]^2} \right)^{1/2}. \end{aligned} \quad (2)$$

These expressions can be derived analogously to how the corresponding expressions for the non-interacting case were derived (in the main paper).

## 2.2 Sparse and random interactions

Here we let the activation rate of each unit be dependent on the state of  $n$  other, randomly selected, units. This means that the activation rates at a particular point in time would typically differ between units but the stop-watch would still be scale invariant if the following rule is used

$$p_i(t) = p \left( 1 + w \frac{m_i(t)}{M} \right). \quad (3)$$

Here  $p_i(t)$  denotes the activation rate of unit  $i$  and  $m_i$  is the number of units “connected” to unit  $i$  that are activated. Also in this case time-intervals of

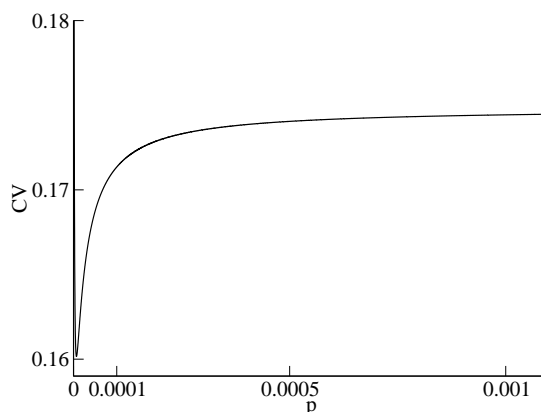


Figure 2: Coefficient of variation for the stop-watch with units connected according to equation 4,  $M=50$  and  $\frac{w}{M} = 0.0000005$

different durations can be encoded by changing  $p$ . Expressions for the distribution of  $T_{f.M}$  can in principle be derived but will depend on the exact way that units interact. Note that neither the sparseness nor the randomness of the interactions will influence the scale invariance.

### 2.3 Additive interactions

We also note that if the interaction is additive, scale invariance will in general not be preserved. Indeed in the case of all-to-all “connectivity” we get the following rule

$$p_c = p + w \frac{m}{M}. \quad (4)$$

That this will not lead to scale invariant behavior can be understood by noting that to encode two different time intervals we change  $p$  but not  $w$  (by assumption). That is, the effect of the interactions is not scale invariant. Of course, if the relevant values of  $p$  are much larger than  $w$ , the system will be approximately time-scale invariant (since it can be approximated well by the unconnected system). Figure 2 illustrates this point, showing that for  $\frac{w}{M} = 0.0000005$  the variations of the CV are small when  $p$  changes one order of magnitude (from  $p = 0.0001$  to  $p = 0.001$ ). The CVs were calculated using the following expressions for the mean and standard deviation of  $T_{f.M}$ , which were derived as the corresponding expressions for the unconnected system.

$$\begin{aligned} E[T_{f.M}] &= \sum_{k=0}^{f.M-1} \frac{1}{(M-k)(p + kw/M)} \\ S[T_{f.M}] &= \left( \sum_{k=0}^{f.M-1} \frac{1}{[(M-k)(p + kw/M)]^2} \right)^{1/2}. \end{aligned} \quad (5)$$

### 3 The effect of noise in the output of the stop-watch units

In demonstrating scale invariance we have assumed that the state of the stop-watch (i.e. the number of units activated at time  $t$ ) is known to the read-out mechanism. This may or may not be the case in a real implementation and it is therefore of interest to investigate the effect of making the stop-watch units noisy (in the sense of not unequivocally signaling their state).

In this section we will consider a case in which the state of one unit is signalled by a realization of a Poisson process of a certain rate. This is as if the stop-watch units were firing action potentials according to a Poisson process with two different rates, one for the spontaneous state and another for the activated state. It is clear that the performance of the stop-watch will depend on the rate difference between the two states. If this difference is very large, the read-out mechanism will never be 'confused' about which state the stop-watch is in and the performance will be identical to the situation without noise in the outputs. If the difference is small, on the other hand, it will be impossible (for any imaginable causal read-out mechanism) to know the state of the stop-watch with certainty. Below we will show data from two cases. The activated state is in both cases associated with a rate of 10 Hz and we will investigate the effect of increasing the rate of the spontaneous state from 0 to 5 Hz.

#### 3.1 The read-out mechanism

In the following we assume that the read-out unit will receive the sum of the outputs from the stop-watch units. Given the Poissonian assumption, the read-out unit will consequently receive a Poissonian spike train with a rate that depends on the state of the stop-watch. For example, if at time  $t$  there are 28 units (of 50, say) activated and the rates are 5 and 10 for the spontaneous and activated states respectively, the read-out unit will 'see' a Poisson spike train of 390 Hz ( $10 \cdot 28 + 22 \cdot 5$ ). To investigate the 'response timing' we need an explicit response rule that determines when the read-out unit should issue a 'response'. We were not aware of any 'standard' procedure for a case such as this, so we came up with the following heuristic device:

- Fix an upper  $\Theta_u$  and a lower  $\Theta_l$  rate-threshold (e.g. 450 and 400 Hz).
- For each 'spike' time, sum the  $z$  previous inter-spike intervals.
- Calculate the likelihood that this sum comes from each of two Poisson processes specified by the two thresholds above. Call these likelihoods  $L(\Theta_u)$  and  $L(\Theta_l)$ .
- Find the first sequence where  $L(\Theta_u) > L(\Theta_l)$  for  $m$  consecutive time-points and take the last of these points as the time-point of the response.

We do not claim that this is the optimal way of testing the hypothesis that the rate of the stop-watch output exceeds a certain level, but it works in practice. It is important to note that this 'response mechanism' was not designed to produce scale invariant responding. The main criteria used was to achieve a monotonous increase in the mean 'response' times and moderate CVs. To use

the sum of the ISIs as the statistic of choice is roughly equivalent to making a local estimate of the firing rate (by for example counting the number of events in a given time window), but it is computationally more efficient. Note that there are four parameters, the two thresholds and, the number of ISIs to sum ( $z$ ) and the length of the sequence where the likelihood of the higher rate should exceed that of the lower ( $m$ ). However, once the rates for the stop-watch unit are decided upon, the upper threshold will be constrained. For example, we know that the variability of the stop-watch is at a minimum when 80% of the units are activated. In terms of the example above this means that we should set the upper threshold at 450 Hz. Once the upper threshold is set the lower threshold is limited by this and some small number. In practice it was chosen so that the difference of the likelihoods was a reasonably smooth curve. That is, if we would choose a lower threshold of 449 this would make the likelihoods almost identical and the difference between the two dominated by sampling noise. The values of the other two parameters were set in order to optimize the detection.

### 3.2 Results

We will show two cases in which the procedure outlined above gave rise to approximately time-scale invariant responses. The firing rate of a stop-watch unit in the activated state was fixed at 10 Hz but in the spontaneous state it could be either 0 or 5 Hz. We used a stop-watch with 50 units and investigated six different values of the activation rate (corresponding to an expected 'response' time of 40 units activated of 1,2,5,10,20, and 50 seconds respectively). For each of these values we first generated one realization of the stop-watch. We then used this realization to generate a Poisson spike train with a rate that changed accordingly. This spike train was then the input to the device outlined above and on each trial a response time was collected. This was repeated 5000 times for each value of the activation rate. Fig. 3 shows the mean response time and the CVs for the two cases corresponding to the two different spiking rates of the spontaneous state. It is clear that the mean response time is increasing as the activation rate decreases, but the relation between the two is no longer described by Eq. 1 in the main text. Indeed the decrease is sub-linear compared to the stop-watch without noise. This slower increase is due to that we use the same value of  $m$  for all values of the activation rates. The read-out procedure is essentially a statistical test that is repeated many times until the null-hypothesis (of that the rate is less than the high threshold) is rejected. For the longer time intervals there are many more opportunities for this to happen before the true rate has reached the right level. To have a more linear increase the parameter  $m$  would need to increase with the length of the interval. We note however that the important thing is that the mean 'response' time *is* increasing monotonously, the rate of the increase is relatively unimportant. Fig. 3 also shows that the CVs are relatively constant in both cases. For the shortest time interval (corresponding to one second in the noise-free model) there is a slight (but significant) deviation. This is presumably an effect of that the rate is changing very fast in this case, so for the large value of  $z$  we used ( $z = 55$ ) there will be ISIs corresponding to many different rates.

We have chosen parameters ( $m$  and  $z$ ) to make the read-out approximately scale invariant. We did not make an exhaustive search over the parameter space and there are most likely parameters for which the system is even more scale

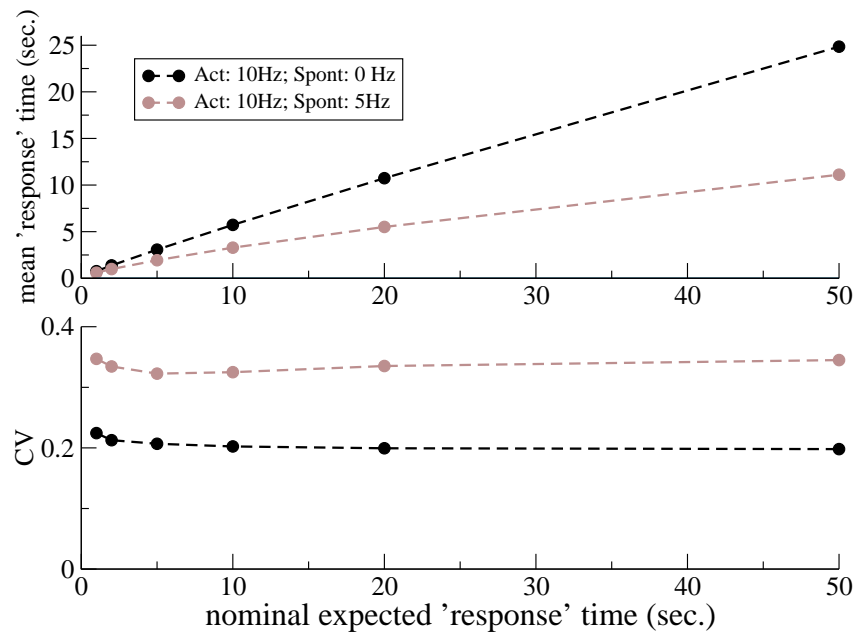


Figure 3: Average 'response' time and CV for the Poisson noise model. Top graph shows the average 'response' time produced by the read-out mechanism outlined in the text. Bottom graph shows the corresponding CVs. Each data point is based on 5000 simulations (trials). The standard errors for the CV data are too small to be seen on the graph. The units of the X-axis are the expected 'response' times of the stop-watch (without noise) with a threshold of 40 activated units. The thresholds were 400 and 300 for the 0 and 10 Hz case and 450 and 400 for the other. The other parameters were  $z = 55$  and  $m = 9$ .

invariant. Of course there are also parameters for which the system will be less scale invariant. However, this example serves to show that the stop-watch can be used to estimate time intervals even if the outputs of the stop-watch units are very noisy.

## 4 The micro-circuit model

Each unit of the model consists of three interconnected neurons. One neuron is modeled using two compartments one corresponding to the soma and axon and one to the dendrites. For neuron  $i$ , the membrane potentials of the soma ( $V_i^s$ ) and dendrites ( $V_i^d$ ) are given by:

$$C_m \frac{dV_i^s}{dt} = -I_{\text{Leak}}(V_i^s) - I_{\text{Na},i} - I_{\text{KDr},i} - g_c \frac{(V_i^s - V_i^d)}{p}$$

$$C_m \frac{dV_i^d}{dt} = -I_{\text{Leak}}(V_i^d) - g_c \frac{(V_i^s - V_i^d)}{1-p} - I_i,$$

where  $C_m = 0.5\mu\text{F}/\text{cm}^2$  is the membrane capacitance,  $p = 0.5$  is the relative area of the somatic membrane and  $g_c = 0.5\text{mS}/\text{cm}^2$  is the conductance between the soma and dendrite. The leak current was  $I_{\text{Leak}}(V) = g_{\text{Leak}}(V - V_{\text{Leak}})$  for both compartments, with  $g_{\text{Leak}} = 0.1\text{mS}/\text{cm}^2$  being the leak conductance and  $V_{\text{Leak}} = -80\text{mV}$  the leak reversal potential. The sodium current ( $I_{\text{Na}}$ ) and the delayed rectifier potassium current ( $I_{\text{KDr}}$ ) were modeled using the Hodgkin-Huxley formalism. The gating variables obey:

$$\frac{dx}{dt} = \Phi_x [\alpha_x(V(1-x) - \beta_x(V)x)] = \Phi_x \frac{x_\infty(V) - x}{\tau_x(V)},$$

where

$$x_\infty(V) = \frac{\alpha_m(V)}{\alpha_m(V) + \beta_m(V)},$$

$$\tau_x(V) = \frac{1}{\alpha_m(V) + \beta_m(V)}$$

and where  $x$  can be  $m$ ,  $h$  or  $n$  and are the activation and inactivation gates. The sodium current is  $I_{\text{Na}} = g_{\text{Na}}m^3h(V - V_{\text{Na}})$ , where  $g_{\text{Na}} = 45\text{mS}/\text{cm}^2$  is the maximal sodium conductance,  $V_{\text{Na}} = 55\text{mV}$  is the sodium reversal potential,

$$\alpha_m = \frac{-0.1(V + 32)}{e^{-(V+32)/10} - 1},$$

$$\beta_m = 4e^{-(V+57)/18},$$

$$\alpha_h = 0.07e^{-(V+48)/20},$$

$$\beta_h = \frac{1}{e^{-(V+18)/10} + 1},$$

and  $\Phi_m = \Phi_h = 2.5$ . The potassium current is  $I_{\text{KDr}} = g_{\text{K}}n^4(V - V_{\text{KDr}})$ , where  $g_{\text{K}} = 18\text{mS}/\text{cm}^2$  is the maximal potassium conductance,  $V_{\text{K}} = -80\text{mV}$  is the potassium reversal potential,

$$\alpha_n = \frac{-0.01(V + 34)}{e^{-(V+34)/10} - 1},$$

$$\beta_n = 0.125e^{-(V+44)/80},$$

and  $\Phi_n = 5$ . All variables having units of electrical potential and time are in units of millivolt and millisecond, respectively.

The input to the dendritic compartment is a sum of one NMDA mediated current due to the recurrent connections and one external current  $I = I_{\text{NMDA}} + I_{\text{ext}}$ , where for the  $i$ th neuron

$$I_{\text{NMDA}i} = \sum_{j=1}^3 g_{\text{NMDA}} s_{ij} \frac{(V_i^d - V_{\text{syn}})}{1 + 0.3[\text{Mg}^{2+}]e^{-0.08V_i^d}},$$

where  $[\text{Mg}^{2+}] = 0.5\text{mM}$  is the magnesium concentration,  $V_{\text{syn}} = 0$ ,  $g_{\text{NMDA}} = 22\mu\text{S}/\text{cm}^2$ ,  $j$  refers to the presynaptic neurons,

$$\frac{ds}{dt} = \alpha_s x(1 - s) - \beta_s s,$$

$$\frac{dx}{dt} = \alpha_x F(V_j^s)(1 - x) - \beta_x x,$$

$$F(V_j^s) = \frac{1}{1 + e^{-V_j^s/2}},$$

$\alpha_s = 1$ ,  $\beta_s = 0.01$ ,  $\alpha_x = 10$  and  $\beta_x = 0.5$  (in 1/ms).

The external input  $I_{\text{ext}}$  was modeled as a constant mean plus a random term,  $I_{\text{ext}} = \mu + \sigma\xi(t)$ . The amplitude of the random term was  $\sigma = 0.25$  and the different values of  $\mu$  used to encode different interval durations are stated in the main paper.